

Effect of drying methods on perovskite films and solar cells

Ling Liu¹, Chuantian Zuo^{1,2,†}, Guang-Xing Liang³, Hua Dong⁴, Jingjing Chang⁵, and Liming Ding^{1,†}

¹Center for Excellence in Nanoscience (CAS), Key Laboratory of Nanosystem and Hierarchical Fabrication (CAS), National Center for Nanoscience and Technology, Beijing 100190, China

²Key Laboratory of Semiconductor Materials Science, Beijing Key Laboratory of Low Dimensional Semiconductor Materials and Devices, Institute of Semiconductors, Chinese Academy of Sciences, Beijing 100083, China

³College of Physics and Optoelectronic Engineering, Shenzhen University, Shenzhen 518060, China

⁴School of Electronic and Information Engineering, Xi'an Jiaotong University, Xi'an 710049, China

⁵Academy of Advanced Interdisciplinary Research, Xidian University, Xi'an 710126, China

Citation: L Liu, C T Zuo, G X Liang, H Dong, J J Chang, and L M Ding, Effect of drying methods on perovskite films and solar cells[J]. *J. Semicond.*, 2024, 45(1), 010501. <https://doi.org/10.1088/1674-4926/45/1/010501>

The high efficiency, solution processibility, and flexibility of perovskite solar cells make them promising candidates for the photovoltaic industry^[1–8]. The deposition method is one of the most critical factors that affect the performance of perovskite films. Various deposition methods have been developed to make perovskite films, including spin-coating, slot-die coating, blade coating, bar coating, spray coating, and screen printing, etc.^[9, 10]. Spin-coating in glovebox is the most widely used method to make perovskite films, but it is hard to make large-area films by using spin-coating, making it not suitable for scalable and automated manufacturing^[11, 12]. Non-spin-coating methods such as blade coating, slot-die coating, spray coating, atomic layer deposition, and vacuum evaporation are more suitable for large-scale manufacturing^[13–19], but these methods need assistance of various equipment which may not be available in many labs. Developing facile preparation methods which do not need complicated equipment would accelerate the industrialization of perovskite solar cells.

In 2019, we developed a facile self-spreading method (modified drop-casting) to make perovskite films^[20]. The self-spreading method produces perovskite films spontaneously without the assistance of coating equipment, making it more suitable for automatic film preparation. What's more, the method is compatible with slot-die coating due to similar drying conditions^[21]. More interestingly, the self-spreading method can yield efficient perovskite solar cells in ambient air without humidity control^[22, 23]. It was also used to make inorganic perovskite films, which show high photovoltaic performance^[24–27]. Recently, it was applied in the fabrication of composition-graded perovskite films^[28, 29]. Our previous works focused on composition optimization and crystallization control of perovskite films made by one-step self-spreading method. The effect of drying conditions on photovoltaic performance of perovskite films made by two-step self-spreading method has not been systematically studied yet.

In this work, we investigated the effect of drying conditions on properties of perovskite films made by a two-step

self-spreading method. Natural drying, vacuum drying, blow drying 1 (self-spreading), and blow drying 2 (soaking) were used to prepare the film in the second step. The effects of drying conditions on film morphology, crystallinity, light absorption, photoluminescence (PL), and photovoltaic performance of perovskite films were studied. A best power conversion efficiency (PCE) of 21.34% is achieved by using vacuum drying.

The perovskite films were made by using two-step self-spreading method^[30] (Fig. 1). For the first step, a $\text{PbI}_2:\text{CsI}$ (molar ratio 35 : 1) film was made by using self-spreading method. For the second step, the $\text{FAI}:\text{MABr}:\text{MACl}$ solution was dropped onto the $\text{PbI}_2:\text{CsI}$ film. We found that the drying conditions in the second step affected the morphology and photovoltaic performance of the resulting perovskite films significantly. Four methods were used to dry the film. The first method is natural drying, i.e. the solution dries naturally without any treatment. The second method is transferring the substrate into a vacuum chamber to dry under vacuum (vacuum drying). The third method is using N_2 blowing to dry the film after self-spreading of the $\text{FAI}:\text{MABr}:\text{MACl}$ solution (blow drying 1). The fourth method is immersing $\text{PbI}_2:\text{CsI}$ film in $\text{FAI}:\text{MABr}:\text{MACl}$ solution and then using N_2 blowing to dry the film (blow drying 2).

The $\text{PbI}_2:\text{CsI}$ film made in the first step contains many holes, which facilitate the penetration of solution and the reaction in the second step (Fig. S1). Fig. S2 shows perovskite films made by different drying methods in the second step. Some rings can be observed in the films made by natural drying, which may be caused by the non-uniform airflow (in the fume cupboard). The rings are almost invisible in the films made by vacuum drying and blow drying. The rings in the film made by natural drying consist of smaller grains with a rougher surface (Fig. S2). The effect of non-uniform airflow can be avoided by using vacuum or blow drying. The top-view scanning electron microscopy (SEM) images measured at the center of the films are shown in Fig. 2. The films made by natural drying, vacuum drying, and blow drying 2 show similar grain size (200–300 nm) and distribution (Figs. 2(a) and 2(c)–2(f)). The film made by blow drying 1 shows much smaller grains (~150 nm). The cross-sectional SEM image of the perovskite film made by natural drying is shown in Fig. S3. The grain size is consistent with the top-view image.

Ultraviolet–visible (UV–Vis) absorption spectra, PL, and X-

Correspondence to: C T Zuo, zuocht@nanoctr.cn; L M Ding, ding@nanoctr.cn

Received 10 OCTOBER 2023; Revised 7 NOVEMBER 2023.

©2024 Chinese Institute of Electronics

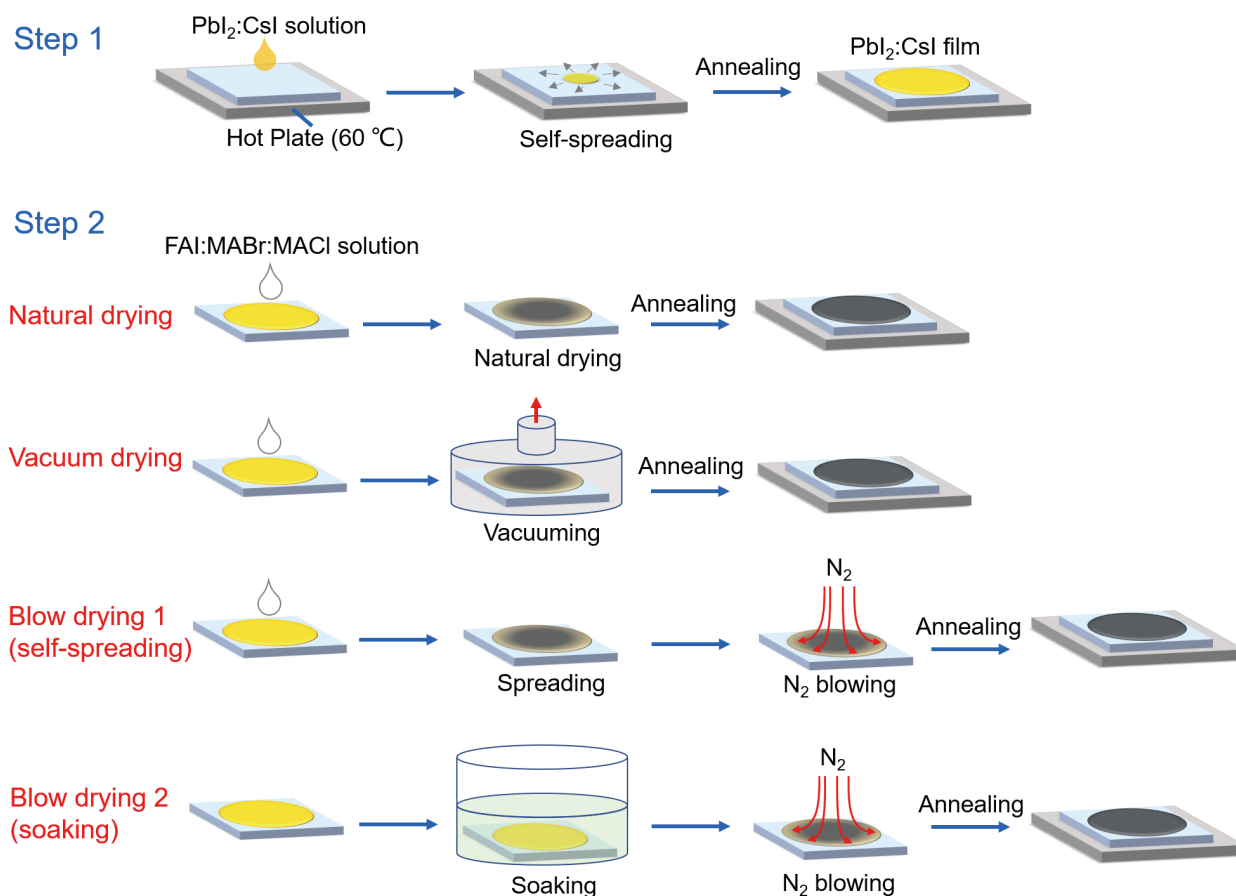


Fig. 1. (Color online) The preparation process for perovskite films and the different drying methods in the second step.

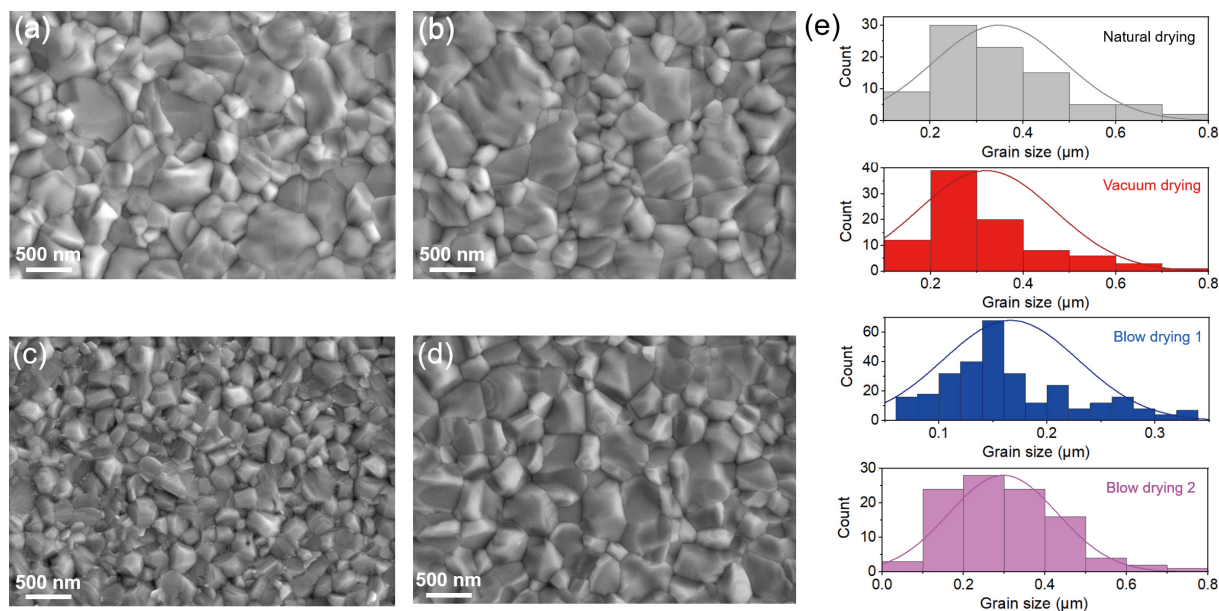


Fig. 2. (Color online) SEM images for perovskite films made by natural drying (a), vacuum drying (b), blow drying 1 (c), and blow drying 2 (d). (e) Distribution of grain size for the perovskite films made by different drying methods.

ray diffraction (XRD) measurements were performed to investigate the effect of drying methods on the optical and crystalline properties of perovskite films. The UV–Vis absorption spectra for the films made by using different drying methods are shown in Fig. 3(a). The absorption spectra for the perovskite films made by natural drying and vacuum drying show slight redshift compared with the films made by blow

drying. The PL peaks for the films made by natural drying and vacuum drying also show slight redshift (Figs. 3(b) and 3(c)), consistent with the absorption spectra. The I : Br ratio in perovskite films has significant effect on their bandgaps^[31–34]. The different drying methods may result in slightly different I : Br ratio in perovskite film, leading to different optical bandgaps and PL peak positions. The film made by blow dry-

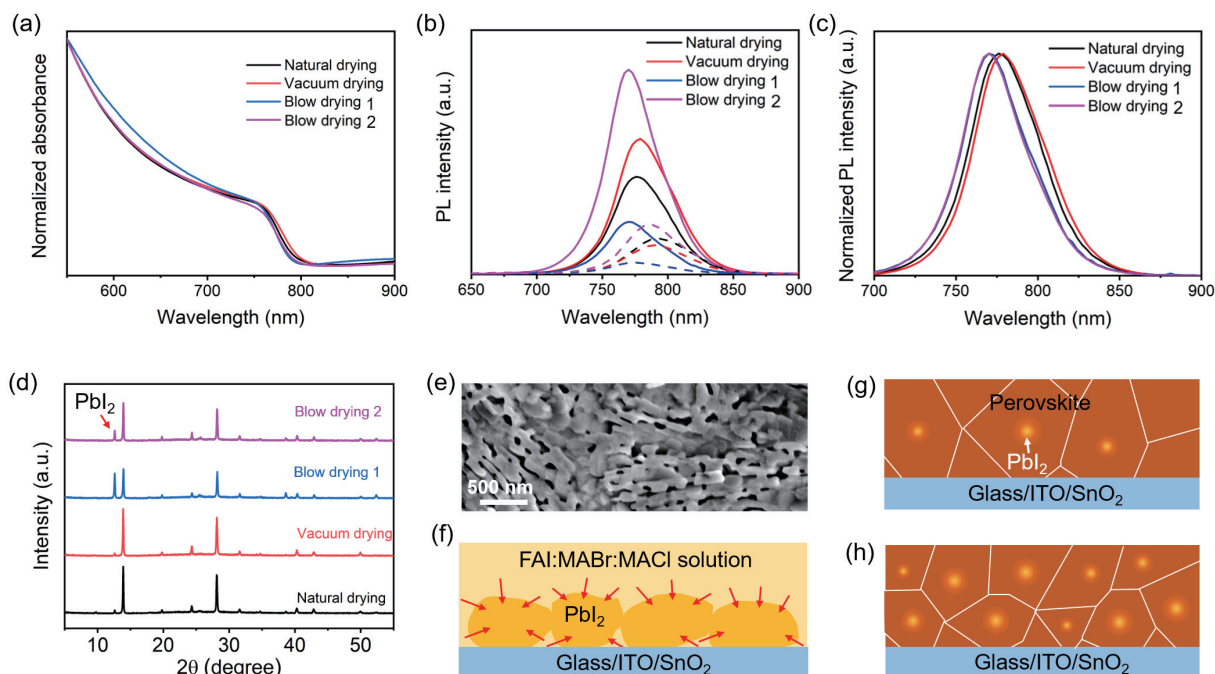


Fig. 3. (Color online) UV-Vis absorption spectra (a), PL spectra (solid line: on glass substrate; dash line: on glass/SnO₂ substrate) (b), normalized PL spectra (on glass substrate) (c), and XRD patterns (d) for the perovskite films made by using different drying methods. (e) SEM image (top view) for PbI₂ film made by self-spreading. (f) Scheme for the reaction between PbI₂ and FAI:MABr:MACl in the second step. (g) Scheme for the perovskite film with large grains and a small amount of unreacted PbI₂. (h) Scheme for the perovskite film with small grains and a large amount of unreacted PbI₂.

ing 1 exhibits a lower PL intensity on glass substrate, which may be due to the defects. The SEM images indicate that the film made by blow drying 1 shows the smallest grains.

All the films show XRD peaks of perovskite phase except one peak at $\sim 12.5^\circ$ for PbI₂ (Fig. 3(d)). The film made by blow drying 1 method shows much higher PbI₂ peak, indicating that the unreacted PbI₂ is more than that in other films. The solution used in the second step can infiltrate into the holes in PbI₂ film (Fig. 3(e)), followed by a reaction between PbI₂ and the halides. The solvent iso-propanol used in the second step can't dissolve PbI₂, so the reaction between PbI₂ and the solutes is driven by the migration of FA⁺, MA⁺, Br⁻, and I⁻ in the film (Fig. 3(f)). When blowing, the drying speed is boosted, and the diffusing of ions into PbI₂ is harder, leading to more unreacted PbI₂ and reduced grain size (Figs. 3(g) and 3(h)). While using blow drying 2 method (soaking), the film contains less unreacted PbI₂. The different results (morphology and PbI₂ residual) for the two blow drying methods may be due to the difference in reactant concentration. For blow drying 1 method (self-spreading), a fixed amount of FAI:MABr:MACl solution is used, and the amount of FAI:MABr:MACl decreases as the reaction proceeds. While the concentration of FAI:MABr:MACl remains constant in the blow drying 2 method (soaking), which facilitates the reaction with PbI₂. So the PbI₂ residual in the film made by blow drying 2 method is less than that in the film made by blow drying 1 method.

Solar cells were made of the perovskite films made by different drying methods (Fig. 4(a)). The cells made by vacuum drying yielded a PCE of 21.34% (Fig. 4(b) and Table 1). The cells made by natural drying and blow drying 2 method (soaking) gave PCEs of 21.17% and 21.18%, respectively. The cells made by blow drying 1 method (self-spreading) gave a PCE

of 19.64%, which is lower than the PCEs for the cells made by other methods (Fig. 4(c)). The decrease in PCE for the cells made by blow drying 1 method (self-spreading) may be due to the unreacted PbI₂ and the small grain size. Too much PbI₂ residual leads to reduced light absorption and lower mobility. The cells made by vacuum drying show a slightly wider photoresponse range (Fig. 4(d)) than the cells made by blow drying 1 method, being consistent with UV-Vis data. Integrated photocurrent of 21.54, 22.49, 21.34, and 21.71 mA/cm² are obtained from the external quantum efficiency (EQE) spectra, being consistent with the *J-V* measurements. The EQE spectra show more obvious difference in the long wavelength region, which is because the absorption coefficient of perovskite for long-wavelength light is much smaller than short-wavelength light. The light absorption of perovskite films can be affected by crystallinity, morphology, and bandgap of perovskite films, which further affect the shape of EQE spectra. The steady-state PCEs for the cells are close to the PCEs obtained from the *J-V* measurements (Fig. S4). The PCE of the cells can be further improved by modifying the SnO₂ layer^[35].

In summary, the effect of drying conditions on properties of perovskite films made by self-spreading, and the photovoltaic performance of perovskite solar cells was investigated. The films made by blow drying 1 method (self-spreading) show smaller grain size and much unreacted PbI₂, which may be due to the fast drying speed. The films made by natural drying, vacuum drying, and blow drying 2 method (soaking) show larger grain size and less unreacted PbI₂, resulting in higher PCE (>21%) than the films made by blow drying 1 method (self-spreading) (19.64%). A PCE of 21.34% was achieved by using vacuum drying method.

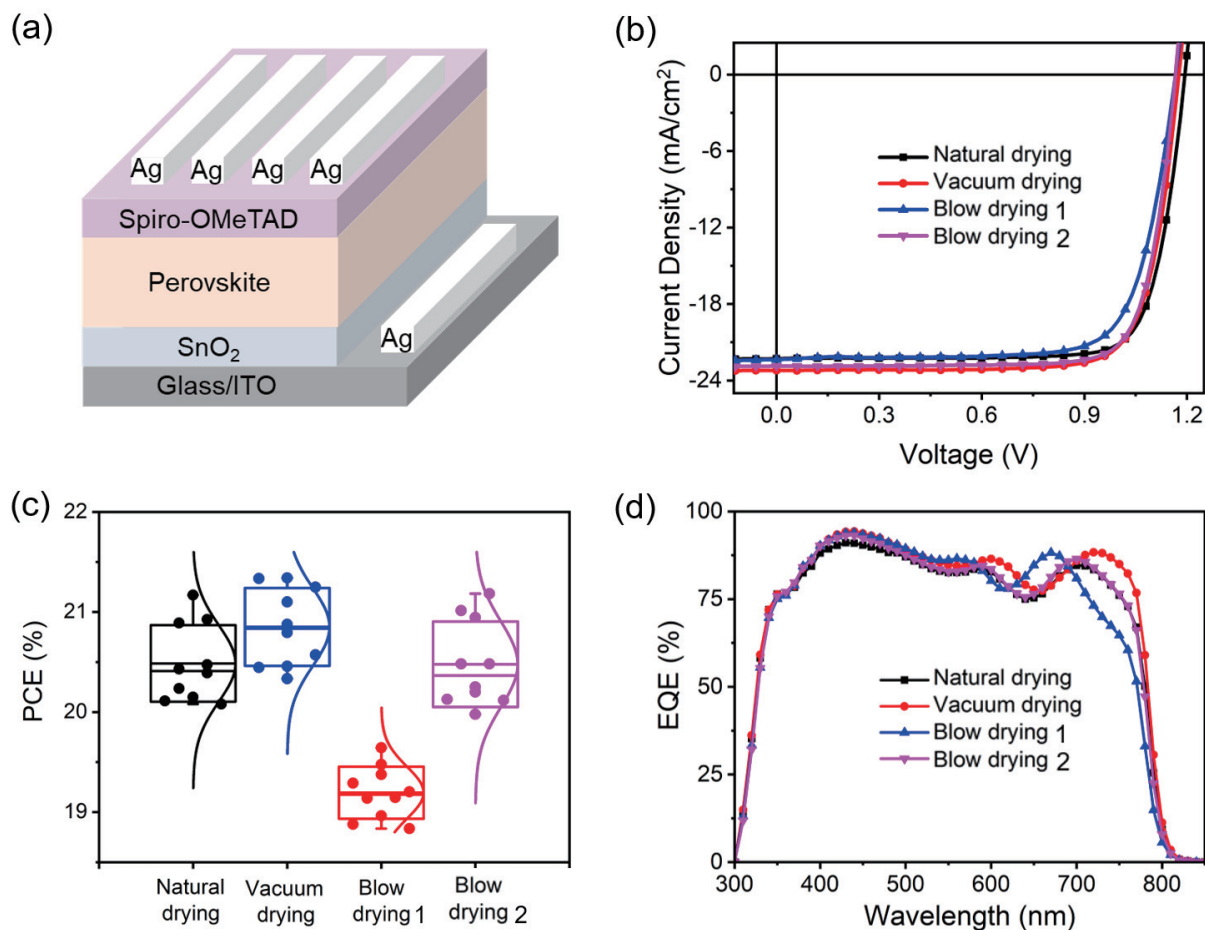


Fig. 4. (Color online) (a) Structure for perovskite solar cells. (b) J - V curves for the cells made by using different drying methods. (c) Distribution of PCE for the cells made by using different drying methods. (d) EQE spectra for the cells.

Table 1. Performance data for solar cells made by using different drying methods.

Drying methods	V_{oc} (V)	J_{sc} (mA/cm ²)	FF (%)	PCE (%)
Natural drying	1.19	22.30	79.51	21.17 (20.49) ^a
Vacuum drying	1.18	23.22	78.15	21.34 (20.85)
Blow drying 1	1.17	22.37	75.26	19.64 (19.11)
Blow drying 2	1.17	22.87	79.41	21.18 (20.48)

^a The PCEs in the brackets are average PCE for 10 devices.

Acknowledgements

We thank the National Natural Science Foundation of China (52203217 and 21961160720), the National Key Research and Development Program of China (2022YFB3803300), and the open research fund of Songshan Lake Materials Laboratory (2021SLABFK02) for financial support.

Appendix A. Supplementary material

Supplementary materials to this article can be found online at <https://doi.org/10.1088/1674-4926/45/1/010501>.

References

- [1] Zhao Y, Ma F, Qu Z H, et al. Inactive (PbI₂)₂RbCl stabilizes perovskite films for efficient solar cells. *Science*, 2022, 377, 531
- [2] Chen X, Guo B, Zhang Z Y, et al. Binary hole transport layer enables stable perovskite solar cells with PCE exceeding 24%. *De-Carbon*, 2023, 1, 100004
- [3] Liu W G, Raza H, Hu X D, et al. Key bottlenecks and distinct contradictions in fast commercialization of perovskite solar cells. *Mater Futures*, 2023, 2, 012103
- [4] Tang G Q, Yan F. Flexible perovskite solar cells: Materials and devices. *J Semicond*, 2021, 42, 101606
- [5] Zhang L X, Pan X Y, Liu L, et al. Star perovskite materials. *J Semicond*, 2022, 43, 030203
- [6] Yang J, Hu J F, Zhang W H, et al. The opportunities and challenges of ionic liquids in perovskite solar cells. *J Energy Chem*, 2023, 77, 157
- [7] Zhou W, Pan T, Ning Z J. Strategies for enhancing the stability of metal halide perovskite towards robust solar cells. *Sci China Mater*, 2022, 65, 3190
- [8] Shao J Y, Li D M, Shi J J, et al. Recent progress in perovskite solar cells: Material science. *Sci China Chem*, 2023, 66, 10
- [9] Ma Y Z, Zhao Q. A strategic review on processing routes towards scalable fabrication of perovskite solar cells. *J Energy Chem*, 2022, 64, 538

- [10] Huang F, Li M J, Siffalovic P, et al. From scalable solution fabrication of perovskite films towards commercialization of solar cells. *Energy & Environ Sci*, 2019, 12, 518
- [11] Yao H H, Shi S H, Li Z Z, et al. Strategies from small-area to scalable fabrication for perovskite solar cells. *J Energy Chem*, 2021, 57, 567
- [12] Jiang Z Y, Wang B K, Zhang W J, et al. Solvent engineering towards scalable fabrication of high-quality perovskite films for efficient solar modules. *J Energy Chem*, 2023, 80, 689
- [13] Castro-Hermosa S, Wouk L, Bicalho I S, et al. Efficient fully blade-coated perovskite solar cells in air with nanometer-thick bathocuproine buffer layer. *Nano Res*, 2021, 14, 1034
- [14] Gu Z K, Wang Y, Wang S H, et al. Controllable printing of large-scale compact perovskite films for flexible photodetectors. *Nano Res*, 2022, 15, 1547
- [15] Li H, Liu M Z, Li M C, et al. Applications of vacuum vapor deposition for perovskite solar cells: A progress review. *iEnergy*, 2022, 1, 434
- [16] Chang X M, Fan Y Y, Zhao K, et al. Perovskite solar cells toward eco-friendly printing. *Research*, 2021, 2021, 9671892
- [17] Zhu Y Q, Hu M, Xu M, et al. Bilayer metal halide perovskite for efficient and stable solar cells and modules. *Mater Futures*, 2022, 1, 042102
- [18] Gao C, Wang H, Wang P, et al. Defect passivation with potassium trifluoroborate for efficient spray-coated perovskite solar cells in air. *J Semicond*, 2022, 43, 092201
- [19] Chen B B, Wang P Y, Ren N Y, et al. Tin dioxide buffer layer-assisted efficiency and stability of wide-bandgap inverted perovskite solar cells. *J Semicond*, 2022, 43, 052201
- [20] Zuo C T, Scully A D, Vak D, et al. Self-assembled 2D perovskite layers for efficient printable solar cells. *Adv Energy Mater*, 2019, 9, 1803258
- [21] Zuo C T, Scully A D, Gao M. Drop-casting method to screen Ruddlesden–Popper perovskite formulations for use in solar cells. *ACS Appl Mater Interfaces*, 2021, 13, 56217
- [22] Zuo C T, Ding L M. Drop-casting to make efficient perovskite solar cells under high humidity. *Angew Chem Int Ed*, 2021, 60, 11242
- [23] Zhang L X, Zuo C T, Ding L M. Efficient MAPbI₃ solar cells made via drop-coating at room temperature. *J Semicond*, 2021, 42, 072201
- [24] Xiao H R, Zuo C T, Zhang L X, et al. Efficient inorganic perovskite solar cells made by drop-coating in ambient air. *Nano Energy*, 2023, 106, 108061
- [25] Xiao H R, Zuo C T, Yan K Y, et al. Highly efficient and air-stable inorganic perovskite solar cells enabled by polylactic acid modification. *Adv Energy Mater*, 2023, 13, 2300738
- [26] Xiao H R, Zuo C T, Liu F Y, et al. Drop-coating produces efficient CsPbI₂Br solar cells. *J Semicond*, 2021, 42, 050502
- [27] Liu L, Xiao H R, Jin K, et al. 4-Terminal inorganic perovskite/organic tandem solar cells offer 22% efficiency. *Nano-Micro Letters*, 2022, 15, 23
- [28] Zuo C T, Tan L G, Dong H, et al. Natural drying yields efficient perovskite solar cells. *DeCarbon*, 2023, 2, 100020
- [29] Zuo C T, Zhang L X, Pan X Y, et al. Perovskite films with gradient bandgap for self-powered multiband photodetectors and spectrometers. *Nano Res*, 2023, 16, 10256
- [30] Liu L, Zuo C T, Ding L M. Self-spreading produces highly efficient perovskite solar cells. *Nano Energy*, 2021, 90, 106509
- [31] Zhang H, Park N G. Progress and issues in p-i-n type perovskite solar cells. *DeCarbon*, 2023, 100025
- [32] Li C, Sun H X, Gan S, et al. Perovskite single crystals: Physical properties and optoelectronic applications. *Mater Futures*, 2023, 2, 042101
- [33] Zhang L X, Li H, Zhang K, et al. Major strategies for improving the performance of perovskite solar cells. *iEnergy*, 2023, 2, 172
- [34] Tao L, Qiu J, Sun B, et al. Stability of mixed-halide wide bandgap perovskite solar cells: Strategies and progress. *J Energy Chem*, 2021, 61, 395
- [35] Tian W J, Song P Q, Zhao Y P, et al. Monolithic bilayered In₂O₃ as an efficient interfacial material for high-performance perovskite solar cells. *Interdiscip Mater*, 2022, 1, 526



Ling Liu got her BS from Sichuan Agricultural University in 2017. Then she joined in Liming Ding Group at National Center for Nanoscience and Technology as a PhD student. Her work focused on organic solar cells, perovskite solar cells and tandem solar cells.



Chuantian Zuo received his PhD in 2018 from National Center for Nanoscience and Technology (CAS). Then he did postdoctoral research in CSIRO, Australia. Currently, he is an associate professor in National Center for Nanoscience and Technology. His research focuses on innovative fabrication techniques for perovskite solar cells.



Liming Ding got his PhD from University of Science and Technology of China (was a joint student at Changchun Institute of Applied Chemistry, CAS). He started his research on OSCs and PLEDs in Olle Inganäs Lab in 1998. Later on, he worked at National Center for Polymer Research, Wright-Patterson Air Force Base and Argonne National Lab (USA). He joined Konarka as a Senior Scientist in 2008. In 2010, he joined National Center for Nanoscience and Technology as a full professor. His research focuses on innovative materials and devices. He is RSC Fellow, and the Associate Editors for Journal of Semiconductors and DeCarbon.